



Enhancement of the parity-violating energy difference of H_2X_2 molecules by electronic excitationNaoya Kuroda, Takumi Oho, and Masato Senami *Department of Micro Engineering, Kyoto University, Kyoto 615-8540, Japan*Ayaki Sunaga *Institute for Integrated Radiation and Nuclear Science, Kyoto University, Osaka 590-0494, Japan*

(Received 3 August 2021; accepted 20 January 2022; published 31 January 2022)

The parity-violating energy difference (PVED) between two enantiomers of a chiral molecule is caused by the weak interaction. Because of the smallness of the PVED, nonzero PVED is yet to be discovered in experimental searches. To detect the PVED, the search for molecules with large PVED values is important. Previously, one of the authors proposed that the PVED may be significantly enhanced in ionized or excited states. The significant enhancement of the PVED in some electronic excited states is proven in this study using H_2X_2 ($X = O, S, Se, Te$) molecules as examples. The maximum enhancement was an about 360-fold increase for H_2Se_2 . For the PVED calculation, we employ the finite-field perturbation theory (FFPT) within the equation-of-motion coupled-cluster theory based on the exact two-component molecular mean-field Hamiltonian. The relation between the enhancement of the PVED and the contribution to the PVED from the highest occupied molecular orbital is also examined. The effects of computational elements, such as parameters related to the electron correlation and FFPT on PVED values in excited states of H_2X_2 molecules, are studied.

DOI: [10.1103/PhysRevA.105.012820](https://doi.org/10.1103/PhysRevA.105.012820)**I. INTRODUCTION**

Parity symmetry is one of the most important concepts in fundamental physics. Some particles are classified by the property under the parity transformation. The pion, for example, has negative parity [1]. The violation of the product of parity and charge conjugation is known to be essential for baryogenesis, which is the process to produce the dominance of matter (baryon) over antimatter (antibaryon) in our universe [2]. Only the weak interaction, among the four fundamental forces (the strong and weak forces, the electromagnetic force, and the gravitation), violates the parity symmetry. For example, the W gauge bosons, W^\pm , interact with the left-handed electron, but not with the right-handed electron. The weak interaction predicts the parity-violating energy difference (PVED) between two enantiomers of a chiral molecule. The possible link between the PVED and the homochirality on the earth is discussed frequently [3–5].

This PVED is demonstrated to be very small for various enantiomers. Quantum chemistry computations can predict this energy and the values are in the range of 10^{-18} to 10^{-12} eV, for H_2X_2 ($X = O, S, Se, Te$) molecules [5–10] and amino acid molecules [11,12]. Many experimental challenges have been proposed for observations of the PVED of chiral molecules. These proposals are related to vibrational-rotational spectroscopy [13], nuclear magnetic resonance (NMR) [14], and so on. However, no PVED signature has been discovered so far. Measurement of the vibrational frequency difference between two enantiomers of the CHF-ClBr molecule [15] yields the most rigorous upper limit. In this experiment, the measured target is not the PVED

in the ground state, but the vibrational frequency difference, and the vibrational frequency difference is suggested to relate the PVED of electronic energy as $E_{el}^{PV}/E_{el} \sim E_{vib}^{PV}/E_{vib}$ [13].

To capture the signature of the PVED, it is important to find molecules with larger PVED. In the paper [6], ionization or electronic excitation of chiral molecules was predicted to enhance the PVED by one order of magnitude or more. This enhancement is due to the breaking of the cancellation between contributions to the PVED from each orbital. Contributions to the PVED from each orbital in chiral molecules are reported to be canceled out by each other [6,10,16], and this was a disappointing feature. However, this cancellation can be a hint to find molecules with the large PVED. The matrix elements of PVED contribution in some orbitals near the highest occupied molecular orbital (HOMO) are larger than the sum of all orbitals. Therefore, ionization or electronic excitation of chiral molecules may disrupt the cancellation and remarkably enhance the PVED. In the work [6], this prediction was checked for the doubly ionized state of the H_2Te_2 molecule. However, the enhancement was only 10% for this ionization.

In the present work, the speculation of the drastic enhancement of the PVED by electronic excitation is confirmed for H_2X_2 ($X = O, S, Se, Te$) molecules by high-accuracy quantum chemical computation of electronic excitation. Excited states were calculated by equation-of-motion coupled-cluster (EOM-CC) theory based on the exact 2-component molecular mean-field (X2Cmmf) Hamiltonian. The enhancement is confirmed by carefully investigating the dependence on the computational method.

H_2X_2 -series molecules are one of the often-used target molecules for the investigation and the test computation of new methodologies because of their simple structure among chiral molecules. The calculations of the electronic structure of H_2X_2 were conducted at various levels of theory: the first report was conducted at the nonrelativistic (NR) level by treating the spin-orbit interaction perturbedly [17], and was followed by the Dirac-Hartree-Fock [10], one-component (1c) [18] and four-component (4c) density functional theory (DFT) [5], and 1c- [19] and 4c-correlation methods [9,20,21]. These 4c calculations are based on Dirac-Coulomb Hamiltonian, and the contribution from the Breit term is also estimated at the 1e-zeroth order regular approximation (ZORA) level within the Breit-Pauli framework [22]. At the MP2 [20] and CCSD(T) [9] levels, calibration studies on the PVED in H_2X_2 molecules were also reported. The calculation of core properties such as the PVED would be sensitive to the correlation procedure, especially the correlation of the core electrons. All calculations above were performed at the electronic ground state of neutral systems.

Quack proposed an experiment in which electronic excited states were employed [23,24] (see, also, reviews [25,26]). In the work, the oscillation between parity eigenstates by the PVED is used for the observation. The initial parity eigenstate of a chiral molecule is created by excitation to and deexcitation from an electronic excited state with an achiral geometry of the molecule. In the course of this proposal, Berger found that the excited state of a formyl fluoride (CHFO) molecule has three times larger PVED than that of the ground state in the same structure of the excited and ground state [27]. In the work, the PVED was calculated by the second-order perturbation theory in the NR framework with spin-orbit interaction, and the denominator of the parity-violating potential has a factor $E_0 - E_i$, where E_0 denotes the energy of the reference state (not necessarily the ground state) and E_i denotes that of an excited state, i . The enhancement of the PVED was explained as follows: The energy of the ground state of a closed-shell chiral molecule is far apart from those of other states, that is, the denominator is large, while the energy of an excited state may be close to those of other states. Our enhancement mechanism arises from a different viewpoint. Our mechanism is motivated by the cancellation between contributions to the PVED from each orbital and is speculated to give orders of magnitude enhancement.

This paper is organized as follows. In the next section, the definition of the PVED is introduced briefly. Then, our computational method and details are described in Sec. III. In Sec. IV, our results are presented. The dependence of the PVED on some parameters of the computations is studied for the H_2O_2 molecule as an example. Then, the enhancement of the PVED by electronic excitation is demonstrated for H_2X_2 molecules. The last section is devoted to our conclusion.

II. THEORY

The PVED dominantly arises from the exchange of Z gauge bosons between electrons and nuclei. The two electron contributions are reported to be subdominant [28]. The Z boson is a massive vector particle, whose mass is about

$91.1876(21)$ GeV/ c^2 [1]. Due to this heaviness, this interaction can be described as a contact interaction. The Hamiltonian density of this contact interaction is expressed as

$$\mathcal{H}(x) = \frac{G_F}{2\sqrt{2}} \bar{\psi}_e(x) \gamma^\mu (g_V^e - g_A^e \gamma_5) \psi_e(x) \times \bar{\psi}_n(x) \gamma_\mu (g_V^n - g_A^n \gamma_5) \psi_n(x), \quad (1)$$

where ψ_e and ψ_n are field operators of the electron and the nucleus, n , $\bar{\psi}_i$ means the Dirac conjugate, $\bar{\psi}_i \equiv \psi_i^\dagger \gamma^0$, γ_5 is defined with gamma matrices as $\gamma_5 = \gamma^5 \equiv i\gamma^0\gamma^1\gamma^2\gamma^3$, and G_F is the Fermi coupling constant, $G_F/(\hbar c)^3 = 1.1663787(6) \times 10^{-5}$ GeV $^{-2}$ [1]. The coordinates of the electron and nuclei are chosen to be the same as $x = x_e = x_n$ since this Hamiltonian represents contact interaction, as explained above. The neutral current couplings of the electron are denoted by $g_V^e = -1 + 4 \sin^2 \theta_W$ and $g_A^e = -1$, where θ_W is the weak-mixing angle, $\sin^2 \theta_W = 0.23121(4)$ [1]. The couplings of nuclei are given by $g_V^n = Z^n(1 - 4 \sin^2 \theta_W) - N^n$ and $g_A^n = Z^n - N^n$, where Z^n and N^n are the number of protons and neutrons in the nucleus, n . Since $(1 - 4 \sin^2 \theta_W)$ is 0.0752, the dominant contribution to g_V^n is the second term, N^n .

The parity-violating contribution is derived as a cross term of V and A parts, that is, the product of g_V^e and $g_A^n \gamma_5$ parts or that of $g_A^e \gamma_5$ and g_V^n parts. The contribution from the former one is studied as the subject of the parity violation in NMR experiments. This contribution is dependent on nuclear spin and, for our X nuclei, isotopes with large natural abundance are singlet. Therefore, the former contribution is neglected in this paper. The latter contribution to the PVED is expressed as follows:

$$\mathcal{H}_{PV}^n(x) = -\frac{G_F}{2\sqrt{2}} g_A^e g_V^n \bar{\psi}_e(x) \gamma^\mu \gamma_5 \psi_e(x) \bar{\psi}_n(x) \gamma_\mu \psi_n(x). \quad (2)$$

This can be reduced to the scalar form in the NR nucleus limit, where the $\mu = 1-3$ components of $\bar{\psi}_n \gamma_\mu \psi_n$ are negligible,

$$\mathcal{H}_{PV}^n(x) \simeq -\frac{G_F}{2\sqrt{2}} g_A^e g_V^n \psi_e^\dagger(x) \gamma_5 \psi_e(x) \psi_n^\dagger(x) \psi_n(x). \quad (3)$$

The parity-violating energy is defined as the integration of the expectation value of this Hamiltonian density,

$$E_{PV} = \int d^3x \langle \Psi | \sum_n \mathcal{H}_{PV}^n(x) | \Psi \rangle, \quad (4)$$

where the ket $|\Psi\rangle$ is a state vector. The PVED, which is the energy difference between enantiomeric pair molecules, is defined as twice the parity-violating energy,

$$\Delta E_{PV} = 2|E_{PV}|. \quad (5)$$

From the viewpoint of this relation, E_{PV} is studied in the following. In this work, the sign of the enhancement is not paid attention to in the following since the PVED has a positive definition.

The interaction length of the weak interaction and the radius of a nucleus are very short, and E_{PV} can clearly be divided

into the contributions from each nucleus,

$$\begin{aligned}
 E_{\text{PV}} &= -\frac{G_F}{2\sqrt{2}} \sum_n g_A^e g_V^n \\
 &\times \left[\int d^3x \langle \Psi | \hat{\psi}_e^\dagger(x) \gamma_5 \hat{\psi}_e(x) \hat{\psi}_n^\dagger(x) \hat{\psi}_n(x) | \Psi \rangle \right] \\
 &= \frac{G_F}{2\sqrt{2}} \sum_n g_V^n M_{\text{PV}}^n. \quad (6)
 \end{aligned}$$

Here, M_{PV}^n parametrizes the contribution from the nucleus n and is defined as

$$M_{\text{PV}}^n \equiv \int d^3x \langle \Psi | \hat{\psi}_e^\dagger(x) \gamma_5 \hat{\psi}_e(x) \hat{\psi}_n^\dagger(x) \hat{\psi}_n(x) | \Psi \rangle. \quad (7)$$

The density distribution of the nucleus is strongly localized and, hence, the contribution of the electron chirality density close to the nucleus, $\langle \Psi | \hat{\psi}_e^\dagger \gamma_5 \hat{\psi}_e | \Psi \rangle$, is dominant for the parity-violating energy.

III. COMPUTATIONAL DETAIL

A. Expectation value

We used the following three methods for the computation of the expectation value of E_{PV} . (i) The analytical one-electron integration at the Hartree-Fock (HF) method. (ii) The Z -vector equation at the coupled-cluster single-double (CCSD) method [8] for the ground state. (iii) The finite-field perturbation theory (FFPT) [29–31] at the CCSD and EOM-CCSD method [21] for the ground and excited states. In the relativistic coupled-cluster framework, the calculations of E_{PV} [9], a P-violating property [32], and parity transformation symmetry (P)-, and time reversal symmetry (T)-violating properties [33–36] using the FFPT method have been reported. In this work, we report the property calculation in excited states at the relativistic EOM-CC level.

In the FFPT method, we calculate the expectation value of a perturbation operator by numerically differentiating the total energy. We first define the total Hamiltonian as follows:

$$\hat{H} = \hat{H}_0 + \lambda \hat{O}, \quad (8)$$

where \hat{H}_0 is the unperturbed Hamiltonian, λ is the perturbation parameter, and \hat{O} is the target operator. In this study, λ and \hat{O} correspond to $\frac{G_F}{2\sqrt{2}} g_V^n$ and $\int d^3x \hat{\psi}_e^\dagger(x) \gamma_5 \hat{\psi}_e(x) \hat{\psi}_n^\dagger(x) \hat{\psi}_n(x)$, respectively. We consider only O, S, Se, and Te for the atom n . From the Hellmann-Feynman theorem, the derivative of the energy can be expressed as follows:

$$\left. \frac{\partial E(\lambda)}{\partial \lambda} \right|_{\lambda=0} = \left\langle \Psi \left| \frac{\partial \hat{H}}{\partial \lambda} \right| \Psi \right\rangle = \langle \Psi | \hat{O} | \Psi \rangle, \quad (9)$$

where Ψ and $E(\lambda)$ are the wave function and the energy with respect to the total Hamiltonian \hat{H} , respectively. Once $\langle \Psi | \hat{O} | \Psi \rangle = M_{\text{PV}}^n$ is derived by this method, E_{PV} can be calculated in Eq. (6).

In this study, we approximated the numerical derivative as follows:

$$\left. \frac{\partial E(\lambda)}{\partial \lambda} \right|_{\lambda=0} \approx \frac{E(\lambda) - E(-\lambda)}{2\lambda}. \quad (10)$$

In this expression, we neglected the contribution from the order beyond $O(\lambda^3)$. To compute M_{PV}^n accurately, the appropriate value of λ was set in our calculation. We note other four sources of errors that the above FFPT procedure leads to: (i) We neglected the contribution of the hydrogen atoms. (ii) Ψ is not the solution of the Hamiltonian \hat{H}_0 because of the much larger value of λ than $\frac{G_F}{2\sqrt{2}} g_V^n$. (iii) The results depend on the value of λ in Eq. (10). (iv) In the numerical derivative, a stricter threshold would be needed than the default setup. The error due to (i) is negligible because the PVED rapidly increases as Z increases, with the ratio scaling roughly as Z^5 [37,38], and g_V^n is small for the hydrogen nucleus (proton). We elucidate the effect of the errors (ii) and (iii) by comparing the results at the FFPT and the Z -vector method in the ground state by using the CCSD method. We elucidate the effect of (iv) by changing the norm of the residual vectors of the EOM-CC calculation. We choose the values of λ referring to the previous study using the FFPT method for the ground state [9].

B. Computational models and parameters

We employed the molecular mean-field approximations [39] to the Dirac-Coulomb-Gaunt (${}^2\text{DCG}_M$) Hamiltonian for the correlated calculations, and the Dirac-Coulomb-Gaunt at the HF levels. For the calculation of the wave function, we used RELCCSD modules at the CCSD [40,41] and EOM-CC [21] levels. (We give the information about the numbers of the correlated electrons and the active space in the next section.) For these computations, we used the DIRAC19 program package [42,43]. We employed Dyall's relativistic basis sets of triple-zeta quality (dyall.ae3z, dyall.v3z) and augmented ones (dyall.aae3z, dyall.acv3z, and dyall.av3z) [44] in the uncontracted form for all atoms. The structure of the molecules was optimized at the HF method for the electronic ground state and dyall.ae2z basis sets at the Dirac-Coulomb Hamiltonian level by utilizing the DIRAC code. For excited states, the same structure was employed to derive all excited-state values in a single calculation. For the optimization computations, Visscher's approximation was used for the two-electron integration of the (SS | SS) class [45]. In Table I, the optimized structures of the H_2X_2 molecules are summarized. The dihedral angle ϕ

TABLE I. Optimized structures of H_2X_2 molecules.

H_2X_2	X-X bond length (Å)	H-X bond length (Å)	H-X-X bond angle (deg)	Dihedral angle ϕ (deg)
H_2O_2	1.390	0.944	103	115
H_2S_2	2.058	1.332	99	90
H_2Se_2	2.333	1.455	97	90
H_2Te_2	2.729	1.650	96	90

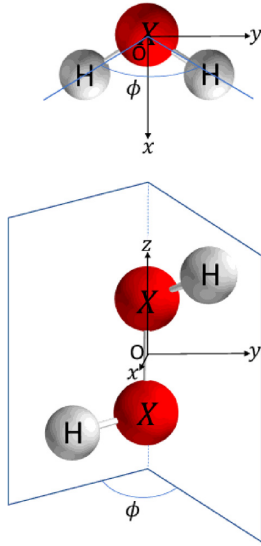


FIG. 1. Definition of the dihedral angle ϕ . The z direction is the direction of the X - X bond and both x , y directions are perpendicular to the X - X bond.

is defined in Fig. 1. The Gaussian charge distribution was employed as the nuclear model for both the nucleus-electron interaction and the nuclear charge density in the PV operator [46]. We set the convergence criterion of the amplitudes of the CC calculations to 10^{-12} , which is the default setting of the DIRAC code. If not stated explicitly, the convergence threshold on the norm of the residual vectors at the EOM-CCSD stage was set to 10^{-10} for the numerical stability of the finite-field calculation.

IV. RESULTS

In this section, we employ the atomic units, that is, Hartree (E_h) to express E_{PV} .

A. Parameter dependence of E_{PV} in H_2O_2

In this section, we investigate the dependence of E_{PV} on the perturbation parameter λ in the FFPT approach by using the H_2O_2 molecule as an example. For more accurate calculations, we should obtain the most suitable λ for each excited state; however, this approach is expensive. A practical approach is using the same λ for all excited states of the

TABLE II. Dependence of E_{PV} on λ within the FFPT method in the electronic ground state of H_2O_2 . The column labeled Dev. represents the relative deviation of the FFPT result from the Z -vector one. The dyall.aae3z basis set was used for all atoms. All electrons were correlated and the virtual spinors were not truncated.

Method	λ (a.u.)	$E_{PV}/10^{-19}E_h$	Dev. (%)
FFPT	1.0×10^{-2}	4.240	2.0
	1.0×10^{-3}	4.110	-1.2
	1.0×10^{-4}	4.306	3.6
	1.0×10^{-5}	2.595	-37.6
Z-vector		4.158	

TABLE III. Dependence of E_{PV} on λ within the FFPT method in the ground (a), first-excited (1a and 1b), and second-excited (2a and 2b) electronic states of H_2O_2 . The dyall.aae3z basis set was used for all atoms. All electrons were correlated and the virtual spinors were not truncated.

λ (a.u.)	State	$E_{PV}/10^{-19}E_h$
1.0×10^{-2}	a	4.240
	1a	-1.956
	1b	12.168
	2a	1381.976
	2b	-17.392
1.0×10^{-3}	a	4.110
	1a	-1.902
	1b	14.800
	2a	1348.683
	2b	-19.839
1.0×10^{-4}	a	4.306
	1a	-0.700
	1b	16.018
	2a	1349.469
	2b	-18.654
1.0×10^{-5}	a	2.595
	1a	-34.637
	1b	-17.931
	2a	1331.494
	2b	-52.569

TABLE IV. Dependence of E_{PV} on the threshold value within the FFPT method in the ground (a), first-excited (1a and 1b), and second-excited (2a and 2b) electronic states of H_2O_2 . The dyall.aae3z basis set was used for all atoms. All electrons were correlated and the virtual spinors were not truncated. The perturbation parameter λ was set to 10^{-3} (a.u.).

Threshold	State	$E_{PV}/10^{-19}E_h$
1.0×10^{-8}	1a	-1.822
	1b	14.882
	2a	1348.893
	2b	-19.762
1.0×10^{-9}	1a	-1.564
	1b	15.129
	2a	1348.887
	2b	-19.488
1.0×10^{-10}	1a	-1.902
	1b	14.800
	2a	1348.683
	2b	-19.839
1.0×10^{-11}	1a	-1.847
	1b	14.845
	2a	1348.806
	2b	-19.771
1.0×10^{-12}	1a	-1.941
	1b	14.760
	2a	1348.785
	2b	-19.878

TABLE V. Dependence of E_{PV} on basis sets within the FFPT method in the ground (a), first-excited (1a and 1b), and second-excited (2a and 2b) electronic states of H_2O_2 . All electrons were correlated and the virtual spinors were not truncated. The perturbation parameter λ was set to 10^{-3} (a.u.).

Basis	State	$E_{PV}/10^{-19}E_h$
dyall.v3z	a	4.155
	1a	-2.527
	1b	16.644
	2a	4163.045
	2b	-21.734
dyall.av3z	a	4.096
	1a	-1.840
	1b	15.054
	2a	1243.297
	2b	-20.008
dyall.ae3z	a	4.162
	1a	-2.546
	1b	16.365
	2a	3790.891
	2b	-21.458
dyall.aae3z	a	4.110
	1a	-1.902
	1b	14.800
	2a	1348.683
	2b	-19.839

same molecule at the EOM-CCSD level after estimating the error of this approach. We also investigate the dependence on the threshold because the FFPT calculation is sensitive to numerical noise. The effects of correlation and diffuse functions of the basis sets on E_{PV} are studied by comparing several basis sets.

Table II demonstrates the dependence of E_{PV} on λ in the FFPT method at the electronic ground state. In the Z -vector calculation, the contribution from the hydrogen was neglected since this contribution was also dropped in the FFPT results. From the table, it is found that the most suitable λ is 1.0×10^{-3} (a.u.) with the difference from the Z -vector calculation, -1.2% . The differences for $\lambda = 1.0 \times 10^{-2}$, 1.0×10^{-4} (a.u.) are similar in magnitude to that of 1.0×10^{-3} (a.u.). When λ is very small, 1.0×10^{-5} (a.u.), the agreement with the reference

value is bad (37.6%). If we employ $\lambda = 1.0 \times 10^{-2}$, 1.0×10^{-4} (a.u.) instead of the most suitable value 1.0×10^{-3} (a.u.), our conclusions about the estimate of the enhancement are unchanged. A too large change beyond the range [that is, 1.0×10^{-5} (a.u.)] may give rise to a too large error. For other H_2X_2 , suitable values of λ are also determined by comparing with the Z -vector results. In the following, $\lambda = 1.0 \times 10^{-3}$, 1.0×10^{-4} , and 1.0×10^{-5} (a.u.) are adopted for H_2S_2 , H_2Se_2 , and H_2Te_2 , respectively. Errors of FFPT values obtained by utilizing these λ are considered to be less than 2% in the valence-correlated calculations, as shown in the next section.

Table III shows the dependence of E_{PV} on λ in the FFPT approach for the electronic excited states of H_2O_2 . The mean values and the standard deviations of E_{PV} in the 1a, 1b, 2a, and 2b states for 1.0×10^{-n} (a.u.) ($n = 2, 3, 4$) are -1.5 ± 0.7 , 14.3 ± 2.0 , 1360.0 ± 19.0 , and -18.6 ± 1.2 (E_h), respectively, where mx represents the m th excited state obeying the x symmetry. The standard deviation for λ is much smaller than the enhancement of E_{PV} , except for state 1a. The value of λ suitable for the ground-state computations was chosen for the following computations of excited states even if it might not be the best. Our purpose is to establish the existence of the enhancement of E_{PV} by two or three orders of magnitude by electronic excitation. Hence, potential error caused by λ does not affect our conclusion. For all λ and even for $\lambda = 1.0 \times 10^{-5}$ (a.u.), E_{PV} in state 2a increases by about 300 times compared to the ground state (a). We will discuss this enhancement later in detail. For state 1a, the standard deviation is a similar order as that of the mean value. However, our purpose is not the accurate computation, and the accuracy of the state with small E_{PV} is not a serious issue. The large difference in E_{PV} by λ in the state with a small E_{PV} is speculated to be caused by numerical noise, and this noise may be prevented by adopting a strict threshold value in some cases.

Next, the dependence of E_{PV} on the threshold value in the EOM-CC calculation is checked and the results are summarized in Table IV. From the table, it is seen that the dependence is much weaker than that on λ in Table III for all excited states. For our purpose of this work, the dependence on the threshold is negligible. Compared to 1.0×10^{-12} (the best case), large deviations are only -2.5% and 2.0% for states 1b and 2b at the threshold 1.0×10^{-9} , respectively. The value of the threshold 1.0×10^{-10} is chosen for computations of E_{PV} in the following computations from the viewpoint of the

TABLE VI. Effect of the active space on E_{PV} in the H_2O_2 molecule. $\lambda = 10^{-3}$ (a.u.) was employed.

Basis	Correlating orbitals	Virtual cutoff / E_h	$E_{PV}/10^{-19}E_h$		$E_{PV}/10^{-19}E_h$			
			(Z -vector)		(FFPT)			
			a	a	1a	1b	2a	2b
dyall.acv3z	2s2p	100	4.12	4.04	-1.98	15.39	892.62	-20.94
		500	4.12	4.05	-1.98	15.37	899.28	-20.93
		All	4.12	4.09	-1.58	15.76	899.68	-20.51
	All	100	4.14	4.12	-1.79	15.07	1208.00	-19.95
		500	4.15	4.11	-1.88	14.81	1343.10	-19.81
		All	4.15	4.08	-2.11	14.59	1348.72	-20.05

TABLE VII. Effect of the active space on E_{PV} in the H_2S_2 molecule. $\lambda = 10^{-3}$ (a.u.) was employed.

Basis	Correlating orbitals	Virtual cutoff / E_h	$E_{PV}/10^{-18}E_h$ (Z vector)		$E_{PV}/10^{-18}E_h$ (FFPT)			
			a	a	1a	1b	2a	2b
dyall.acv3z	3s3p	10	-1.38	-1.40	354.63	358.98	32.21	-36.67
		100	-1.38	-1.39	355.19	359.49	32.23	-36.66
		1000	-1.38	-1.40	355.17	359.47	32.20	-36.69
	2s2p3s3p	10	-1.35	-1.40	365.01	369.10	32.71	-37.23
		100	-1.31	-1.38	368.86	372.41	32.64	-37.83
		1000	-1.31	-1.38	368.94	372.48	32.65	-37.87

balance between the accuracy and computational cost, where the deviations from the results of 1.0×10^{-12} are less than 1%. For other X atoms, a larger threshold is speculated to be safely acceptable since larger spin-orbit interaction gives larger E_{PV} .

Finally, we study the contributions of the correlation and diffuse functions of the basis sets. The significance of the correlation and diffuse functions is shown in Table V. All basis sets in these calculations are the same quality, dyall triple-zeta basis sets, and correlation and diffuse functions are different. From the comparison between the values of dyall.av3z and dyall.aae3z, a large difference is found at state 2a, -8.5%. Hence, correlation functions even for core electrons may affect the accuracy. It is well known that diffuse functions play an important role in the calculations of electronic excited states, and it is significantly important in our study. In the comparison between results in state 2a of dyall.ae3z and dyall.aae3z, the value of the former is about three times that of the latter. This is also seen for the comparison between the results of dyall.v3z and dyall.av3z. Hence, correlation and diffuse functions are important for our study. For other X atoms, computations with the dyall.aae3z basis set are expensive. Hence, the dyall.acv3z basis set is adopted for our computations from the accuracy and computational cost perspectives. (For the oxygen atom, the dyall.acv3z basis set is the same as the dyall.aae3z basis set.)

B. Enhancement of E_{PV} of H_2X_2

In this section, we numerically verify the enhancement of E_{PV} of H_2X_2 in electronic excited states. For H_2S_2 , H_2Se_2 , and H_2Te_2 , the number of correlated electrons and the size of the active space were limited in our computations. It is checked how these truncations affected the accuracy by the comparison between the results of the EOM-CC calculation.

It is also useful to estimate the accuracy of the calculation of larger molecules, where the active space and the correlated electrons are limited. The values of E_{PV} of the H_2O_2 , H_2S_2 , H_2Se_2 , and H_2Te_2 molecules are summarized in Tables VI, VII, VIII, and IX, respectively. The value of λ for H_2X_2 was chosen so that the result with the chosen λ is very consistent with the value by the Z-vector method. The difference of H_2S_2 with the 2s2p3s3p correlation is about 5%, although $\lambda = 10^{-3}$ (a.u.) works well for 3s3p correlated calculations. This small inconsistency is not taken seriously because the best λ for the ground state is not the best one for excited states.

First, we focus on the enhancement of E_{PV} due to the excitation of the electron. In Tables VI-IX, the most enhanced values with the most reliable computational condition are represented in italics. The most reliable computational condition was determined based on the effect of the virtual truncation and the correlated electrons, which are discussed later. The ratios of the most enhanced values to those in the ground states (Z-vector) with the same computational condition are 324, -284, -363, and -130 for H_2O_2 , H_2S_2 , H_2Se_2 , and H_2Te_2 , respectively. These results clearly confirm the significant enhancement of E_{PV} due to the electronic excitation. The enhancement of E_{PV} is much larger than the expected errors discussed in the previous section. In H_2O_2 , the most enhanced state is 2a, while for H_2S_2 , H_2Se_2 , and H_2Te_2 , the most enhanced states are 1a and 1b. One may find E_{PV} of the excited state of a lighter system (e.g., H_2O_2) is larger than that in the ground state of a heavier system (e.g., H_2S_2 and H_2Se_2). However, this comparison is unfair because the dihedral angle of H_2O_2 in the optimized geometry is different from other molecules. It is well known that the values of the PVED are close to zero at $\phi = 90^\circ$ [5-11, 19, 20, 47], which is the optimized dihedral angle for H_2S_2 , H_2Se_2 , and H_2Te_2 . We will discuss this point in detail in the next section.

TABLE VIII. Effect of the active space on E_{PV} in the H_2Se_2 molecule. $\lambda = 10^{-4}$ (a.u.) was employed.

Basis	Correlating orbitals	Virtual cutoff / E_h	$E_{PV}/10^{-17}E_h$ (Z vector)		$E_{PV}/10^{-17}E_h$ (FFPT)			
			a	a	1a	1b	2a	2b
dyall.acv3z	4s4p	20	-8.08	-8.10	2204.80	2107.95	168.99	-506.46
		100	-8.06	-8.09	2204.94	2108.05	168.96	-506.56
	3d4s4p	20	-6.42	-6.49	2281.62	2161.32	167.43	-545.41
		100	-6.28	-6.35	2281.18	2158.49	167.56	-548.84

TABLE IX. Effect of the active space on E_{PV} in the H_2Te_2 molecule. $\lambda = 10^{-5}$ (a.u.) was employed.

Basis	Correlating Orbitals	Virtual cutoff / E_h	$E_{PV}/10^{-15}E_h$ (Z-vector)		$E_{PV}/10^{-15}E_h$ (FFPT)			
			a	a	1a	1b	2a	2b
dyall.acv3z	5s5p	10	-2.23	-2.22	227.66	235.53	27.68	-103.94
		190	-2.22	-2.23	227.67	235.54	27.71	-103.96
	4d5s5p	10	-1.87	-1.88	233.61	240.93	30.39	-114.48
		50	-1.85	-1.88	233.97	241.42	30.65	-115.37

Next, we discuss the effects of the number of the correlated electrons and the size of the active space on E_{PV} in excited states. The effect of the virtual truncation is less than 1%, except for H_2O_2 . In the case of H_2O_2 , E_{PV} is sensitive to truncation, while this feature is not found at the ground state. For example, the error of 100 E_h cutoff from the non-cutoff value is about 12% at state 2a when all electrons are correlated. Nevertheless, the truncation of the virtual space does not change the magnitude of the enhancement of E_{PV} significantly. Hence, the use of the small active space is sufficient for the simple estimate of E_{PV} , especially for large systems.

For H_2S_2 , H_2Se_2 , and H_2Te_2 , the effect of the correlation of core-valence orbitals is roughly within a few % for almost all excited states, and contributions are about 10% in state 2b of H_2Se_2 and H_2Te_2 . These contributions are smaller than those in the ground states of H_2Se_2 and H_2Te_2 , which are about 30% and 20%, respectively. The situation is different in the case of H_2O_2 . The contribution of the correlation of the 1s orbital to E_{PV} is found to be 33% at state 2a. Hence, the contribution of the core-valence correlation to E_{PV} depends on molecules. Nevertheless, for state 2a of H_2O_2 , the enhancement of E_{PV} can be reproduced even in 2s2p correlated computations. This result encourages us to apply our methodology to large systems, where correlated electrons and the active space are inevitably limited.

C. Mechanism of enhancement of the PVED

We have confirmed the significant enhancement of E_{PV} in the electronic excited state compared to the ground state. We should pay attention to the difference of the dihedral angle between H_2O_2 and others. The former is 115° , while the other

is 90° , respectively. Particularly, it is known that the PVED is almost zero around 90° . To clarify how the enhancement occurs, we compare the results for the optimized structure with those at $\phi = 45^\circ$, where it is one of the most typical targets of the study of the PVED because of its extremum value of the PVED.

We summarize the values of E_{PV} in the optimized and $\phi = 45^\circ$ structures in Table X. To derive the structure with $\phi = 45^\circ$, other angles and lengths were fixed on the optimized structure. For $\phi = 45^\circ$, most values of E_{PV} in excited states are the same order as the ground state, though the values are increased slightly. One important observation is that the maximum E_{PV} in the excited states of the optimized structure is larger than that in the $\phi = 45^\circ$ structure for all H_2X_2 by one or two orders of magnitude. Amazingly, E_{PV} in state 2a of H_2O_2 in the optimized structure ($1.35 \times 10^{-16}E_h$) is larger than that in the ground state of H_2S_2 in the $\phi = 45^\circ$ structure ($-1.68 \times 10^{-17}E_h$), despite the well-known Z-scaling rule of the PVED, which was first reported in the 1970s [37,38].

Finally, the enhancement is studied by the contribution, $M_{PV}^{n,i}$, from the i th orbital to the matrix element of M_{PV}^n . The contributions from the i th pair of spinors (Kramers pairs) $2M_{PV}^{n,i}$ and the accumulated total value in the optimized and $\phi = 45^\circ$ structures are shown in Figs. 2–5. The contributions were calculated by the HF method. In the figures, the values of $2M_{PV}^{n,i}$ from HOMO to HOMO – 5 in the optimized structure are larger than those in the $\phi = 45^\circ$ structure for almost all cases. HOMO and HOMO – 1 give the largest two $M_{PV}^{n,i}$ in H_2X_2 , except for H_2O_2 , while for H_2O_2 , HOMO – 4 and HOMO – 5 give the largest two values. Despite large $M_{PV}^{n,i}$, the total E_{PV} in the ground state of the optimized structure of all H_2X_2 is small because most of them cancel out each other.

 TABLE X. E_{PV} for the optimized and $\phi = 45^\circ$ structures of the H_2X_2 molecules.

H_2X_2	Structure	Correlating orbitals	Virtual cutoff / E_h	E_{PV}/E_h (FFPT)				
				a	1a	1b	2a	2b
H_2O_2	opt ($\phi = 115^\circ$)	All	All	4.08×10^{-19}	-2.11×10^{-19}	1.46×10^{-18}	1.35×10^{-16}	-2.01×10^{-18}
	$\phi = 45^\circ$			-3.45×10^{-19}	1.99×10^{-18}	1.74×10^{-18}	1.99×10^{-18}	2.71×10^{-19}
H_2S_2	opt ($\phi = 90^\circ$)	2s2p	100	-1.38×10^{-18}	3.69×10^{-16}	3.72×10^{-16}	3.26×10^{-17}	-3.78×10^{-17}
	$\phi = 45^\circ$			-1.68×10^{-17}	1.80×10^{-17}	3.55×10^{-17}	3.76×10^{-17}	4.01×10^{-17}
H_2Se_2	opt ($\phi = 90^\circ$)	4s4p	100	-8.10×10^{-17}	2.20×10^{-14}	2.11×10^{-14}	1.69×10^{-15}	-5.07×10^{-15}
	$\phi = 45^\circ$			-1.63×10^{-15}	1.31×10^{-15}	2.13×10^{-15}	2.28×10^{-15}	1.64×10^{-15}
H_2Te_2	opt ($\phi = 90^\circ$)	5s5p	70	-2.23×10^{-15}	2.28×10^{-13}	2.36×10^{-13}	2.77×10^{-14}	-1.04×10^{-13}
	$\phi = 45^\circ$			-2.72×10^{-14}	1.23×10^{-14}	3.14×10^{-14}	3.08×10^{-14}	1.79×10^{-14}

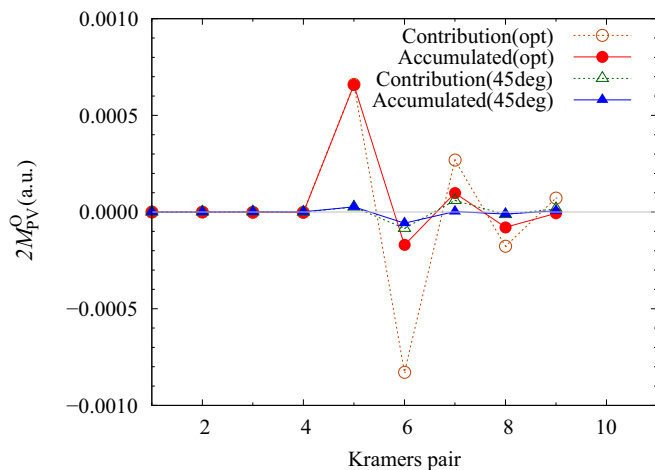


FIG. 2. Contribution to M_{PV}^O from each Kramers pair and accumulated value for H_2O_2 in the ground state of the optimized and $\phi = 45^\circ$ structures.

From these figures, it is speculated that the total E_{PV} increases significantly if the electron in the orbital with a large $M_{PV}^{n,i}$ is excited. (Here, we simply ignore other contributions, e.g., $M_{PV}^{n,i}$ of the virtual orbital to which the electron is excited, and the change of the reference from the HF to the CCSD at the EOM-CC level.) We analyze the R vector of the EOM-CC calculation, which describes the excitation from the CC wave function, for the most enhanced states in Table X. It is found that the excitation from the HOMO accounts for more than 85%, except for H_2S_2 in the 45° structure and H_2O_2 in the optimized structure. For H_2S_2 in the 45° structure, the contribution of the excitation from the HOMO is about 73%. For H_2O_2 in the optimized structure, any dominant contribution larger than 50% does not exist and many excitations contribute to the excited state. The contribution of the excitation from the HOMO is 38%. Table XI shows the comparison between the total E_{PV} for the states in italicized letters in Table X and the contribution from the HOMO in the ground state. For excited

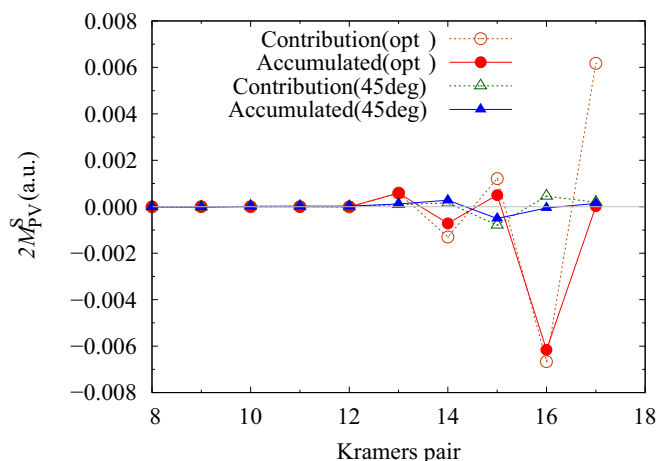


FIG. 3. Contribution to M_{PV}^S from each Kramers pair and accumulated value for H_2S_2 in the ground state of the optimized and $\phi = 45^\circ$ structures.

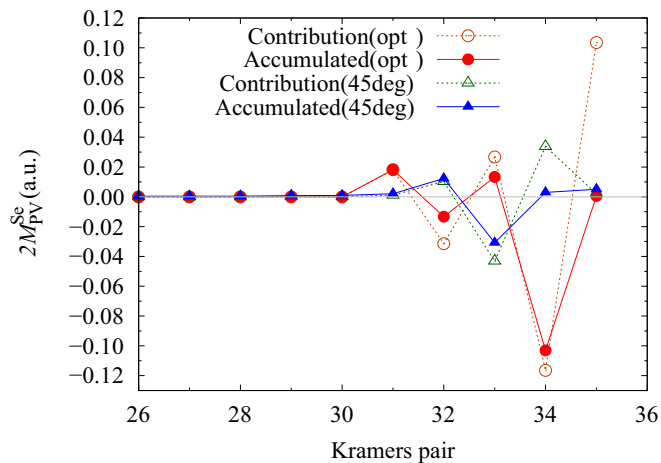


FIG. 4. Contribution to M_{PV}^{Se} from each Kramers pair and accumulated value for H_2Se_2 in the ground state of the optimized and $\phi = 45^\circ$ structures.

states of the optimized geometry, the HOMO's value is of the order of that of the total E_{PV} of H_2X_2 , except for H_2O_2 , and the sign of the PVED is opposite to the contribution from the HOMO. For the $\phi = 45^\circ$ structure, the values of the HOMO are smaller than or comparable to the total E_{PV} in the ground state. It would be the reason for the small enhancement in the excited state. Accordingly, the magnitude of the maximum enhancement of E_{PV} in the excited state may be estimated by the $M_{PV}^{n,i}$ of the orbital from which the electron is excited. In Table XI, for H_2O_2 , E_{PV} is much larger than that expected from the HOMO's value. More detailed analysis is required for the explanation of this enhancement.

We computed the matrix elements of E_{PV} of all virtual orbitals of H_2O_2 in the optimized structure, to which the electron is excited. All these contributions are less than the contribution from the HOMO and cannot explain the enhancement for H_2O_2 . We speculate that the modification of molecular orbitals from the HF orbitals explains the enhancement. This relaxation effect cannot be checked in the computations in

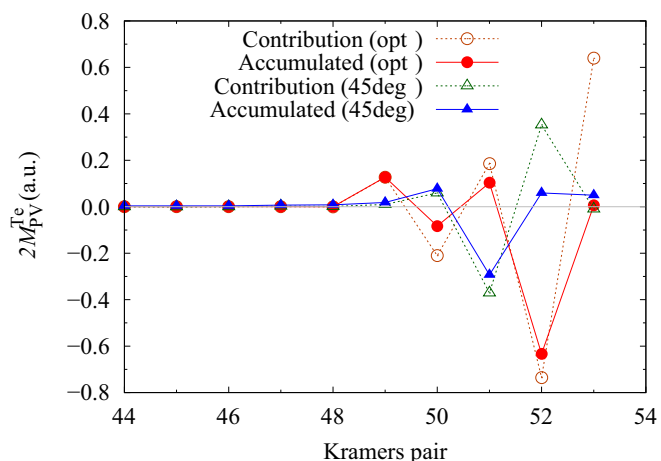


FIG. 5. Contribution to M_{PV}^{Te} from each Kramers pair and accumulated value for H_2Te_2 in the ground state of the optimized and $\phi = 45^\circ$ structures.

TABLE XI. The total E_{PV} and the contribution from the HOMO in the H_2X_2 molecules. The excited-state (ES) values of E_{PV} are those in the excited states shown in italics in Table X.

H_2X_2	Structure	E_{PV}/E_h (a)	E_{PV}/E_h (ES)	E_{PV}/E_h (HOMO)
H_2O_2	opt ($\phi = 115^\circ$)	4.08×10^{-19}	1.35×10^{-16}	-4.21×10^{-18}
	$\phi = 45^\circ$	-3.45×10^{-19}	1.99×10^{-18}	-9.93×10^{-19}
H_2S_2	opt ($\phi = 90^\circ$)	-1.38×10^{-18}	3.72×10^{-16}	-7.20×10^{-16}
	$\phi = 45^\circ$	-1.68×10^{-17}	4.01×10^{-17}	-2.25×10^{-17}
H_2Se_2	opt ($\phi = 90^\circ$)	-8.10×10^{-17}	2.20×10^{-14}	-3.54×10^{-14}
	$\phi = 45^\circ$	-1.63×10^{-15}	2.28×10^{-15}	-7.30×10^{-16}
H_2Te_2	opt ($\phi = 90^\circ$)	-2.23×10^{-15}	2.36×10^{-13}	-3.73×10^{-13}
	$\phi = 45^\circ$	-2.72×10^{-14}	3.14×10^{-14}	5.59×10^{-15}

this work. The relaxation of the HF-occupied orbitals due to the excitation, which leads to the change of the matrix element of E_{PV} , would be estimated by using the average-of-configuration method.

Next, we study the properties of excited states with large enhancement of E_{PV} . In Table XII, we show the excitation energy of the H_2X_2 molecules for the optimized and $\phi = 45^\circ$ structures. Approximate triplet states are formed by the 1a, 2a, and 1b states, except for H_2O_2 , where the 1a, 1b, and 2b states constitute the approximate triplet state. The 2b state in the optimized structures of H_2X_2 , except for H_2O_2 , and the $\phi = 45^\circ$ structure of H_2O_2 forms an approximate triplet with the 3a and 3b states, which is confirmed by our EOM-CCSD computations for the excitation energy. The 2a state of H_2O_2 in the optimized structure forms another triplet state with the 3a and 3b states. The other 2b state in the $\phi = 45^\circ$ structure of the other H_2X_2 is an approximate singlet state. The energy of the ground state of H_2X_2 is apart from those of the excited states, and the energy of the excited state is close to those of other states. Two values of E_{PV} in the same triplet are close to each other and within several percent, except for the optimized structure of H_2O_2 . The other value in the triplet is smaller. Particularly for the optimized structure, even for H_2O_2 , this value is much smaller and about 1/10. The spectrum of the excited states of H_2O_2 is different from that of the others. This difference is considered to originate mainly in the difference of the structure; however, since the spectrum difference is also seen in the $\phi = 45^\circ$ structure, other differences, such as molecular orbitals, may affect the spectrum.

To study the difference in the enhancement between H_2O_2 and H_2X_2 , the Mulliken charge of the HOMO is studied. The HOMO of H_2O_2 in the optimized structure dominantly consists of p_x orbitals of O atoms (86%) and the contributions of p_y and p_z of O atoms are 5% and 6%, respectively. On the other hand, the largest contribution to the HOMO of H_2X_2 in the optimized structure is from p_y orbitals of X atoms. The proportions are smaller for heavier X elements and 62%, 53%, and 49% for $X = S, Se,$ and Te , respectively. The contributions of p_x are the second largest and 24%, 31%, and 38% for $X = S, Se,$ and Te , respectively.

V. CONCLUSION

In this paper, the significant enhancement of the PVED ($=2|E_{PV}|$) by electronic excitation, which was predicted in Ref. [6], has been verified for H_2X_2 by accurate computations based on EOM-CC theory. The ratio of the most enhanced E_{PV} to that in the ground state is 324, -284 , -363 , and -130 for H_2O_2 , H_2S_2 , H_2Se_2 , and H_2Te_2 , respectively. It was predicted that electronic excitation or ionization breaks the cancellation between large contributions to the PVED from orbitals and then E_{PV} is enhanced [6]. The enhancement has been carefully confirmed by checking the dependence on computational parameters, and so on. In the FFPT calculation, the suitable value of the perturbation parameter λ should be employed for each excited state, while in this work, the value of λ is determined by comparing results with those obtained by the Z-vector method. We have confirmed that this

 TABLE XII. Excitation energy for the optimized and $\phi = 45^\circ$ structures of the H_2X_2 molecules.

H_2X_2	Structure	Correlating orbitals	Virtual cutoff / E_h	Excitation energy (eV) (EOM-CCSD)			
				1a	1b	2a	2b
H_2O_2	opt ($\phi = 115^\circ$)	All	All	5.84	5.84	6.78	5.84
	$\phi = 45^\circ$			5.41	5.41	5.41	5.94
H_2S_2	opt ($\phi = 90^\circ$)	$2s2p$	100	4.31	4.31	4.31	4.40
	$\phi = 45^\circ$			3.45	3.45	3.45	4.05
H_2Se_2	opt ($\phi = 90^\circ$)	$4s4p$	100	3.52	3.53	3.54	3.61
	$\phi = 45^\circ$			2.79	2.79	2.79	3.31
H_2Te_2	opt ($\phi = 90^\circ$)	$5s5p$	70	2.86	2.87	2.88	2.95
	$\phi = 45^\circ$			2.26	2.29	2.27	2.69

approach is sufficient for our purpose because the dependence on λ is much smaller than the enhancement of E_{PV} . In the choice of basis sets, it has been reported that both correlation and diffuse functions are essential to computations of E_{PV} in excited states. Diffuse functions are important for ordinary excited-state computations and crucial for the computation of the PVED. E_{PV} in state 2a with the dyall.ae3z basis set is three times as large as that with dyall.aae3z. The PVED in excited states is unaffected by the truncation of active space and the correlation of core-valence orbitals, except for H_2O_2 . The difference between different truncations is within 1%. The deviation by different correlations of core-valence orbitals is within 3% for almost all excited states, while this deviation is about 30% and 20% in the ground states of H_2Se_2 and H_2Te_2 , respectively. In H_2O_2 , the difference by the truncation was about 12% in the largest case, and the contribution of the correlation of the $1s$ orbital is about 33.3% in state 2a. Nevertheless, the enhancement of E_{PV} is much larger than the expected errors discussed in this paper. Although our results for H_2O_2 are sensitive to the choice of active space and correlation orbitals, it is almost insensitive for other H_2X_2 . From the above consideration, it is encouraged that our methodology be applied to large systems, such as chiral molecules with heavy elements and amino acid molecules. From the study of the contribution to the PVED from each orbital, it has been speculated that E_{PV} is remarkably enhanced if electrons are excited from the orbital with a large contribution which is canceled out with contributions from other orbitals. The contribution to E_{PV} from the HOMO in the ground state of the optimized structure have a similar size to the total E_{PV} in the most enhanced excited states, which are primarily dominated by the electrons excited from the HOMO, except for H_2O_2 .

Hence, we have proposed the hypothesis that the maximum enhancement of E_{PV} by electronic excitation can be estimated by the contribution to E_{PV} from the orbital from which the electron is excited. This speculation is true for H_2X_2 , except for H_2O_2 , while the enhancement in H_2O_2 is much larger than the expected value from our hypothesis. Hence the enhancement mechanism in H_2O_2 is considered to be different, and we speculate that the enhancement in H_2O_2 is due to the relaxation, i.e., the modification of molecular orbitals from the HF orbitals by the excitation, since the values of $M_{PV}^{n,i}$ of virtual orbitals, to which the electron is excited, are small.

The significant enhancement found in this work is speculated to occur for other chiral molecules. The enhancement of the PVED by the electronic excitation originates in the breaking of the cancellation between large contributions from orbitals. This cancellation in the ground state is the generic property for most chiral molecules, as discussed in Ref. [5]. Therefore, this enhancement may be the key to discovering the imprint of the weak interaction in chiral molecules experimentally.

ACKNOWLEDGMENTS

This work was supported by JSPS and MEXT Grants-in-Aid for Scientific Research (Grants No. 17K04982, No. 19H05103, and No. 21H00072). A.S. acknowledges financial support from the Japan Society for the Promotion of Science (JSPS) KAKENHI Grants No. 20K22553 and No. 21K14643. We are also thankful for use of the supercomputer of ACCMS (Kyoto University) for the main calculation and Research Institute for Information Technology, Kyushu University (General Projects).

-
- [1] P. A. Zyla *et al.* (Particle Data Group), *Prog. Theor. Expt. Phys.* **2020**, 083C01 (2020).
- [2] E. W. Kolb and M. S. Turner, *The Early Universe* (Westview Press, Boulder, Colorado, 1994).
- [3] For example, see U. Meierhenrich, *Amino Acids and the Asymmetry of Life* (Springer-Verlag, Berlin, 2008).
- [4] J. K. Laerdahl, R. Wesendrup, and P. Schwerdtfeger, *ChemPhysChem* **1**, 60 (2000); A. J. MacDermott, G. O. Hyde, and A. J. Cohen, *Origins Life Evol. Biosphere* **39**, 439 (2009).
- [5] R. Bast, A. Koers, A. S. P. Gomes, M. Iliaš, L. Visscher, P. Schwerdtfeger, and T. Saue, *Phys. Chem. Chem. Phys.* **13**, 864 (2011).
- [6] M. Senami and K. Ito, *Phys. Rev. A* **99**, 012509 (2019).
- [7] M. Senami, K. Inada, K. Soga, M. Fukuda, and A. Tachibana, *Prog. Theor. Chem. Phys.* **31**, 95 (2018).
- [8] A. Shee, L. Visscher, and T. Saue, *J. Chem. Phys.* **145**, 184107 (2016).
- [9] J. Thyssen, J. K. Laerdahl, and P. Schwerdtfeger, *Phys. Rev. Lett.* **85**, 3105 (2000).
- [10] J. K. Laerdahl and P. Schwerdtfeger, *Phys. Rev. A* **60**, 4439 (1999).
- [11] M. Senami and T. Shimizu, *Phys. Lett. A* **384**, 126796 (2020).
- [12] A. J. MacDermott, T. Fu, G. O. Hyde, R. Nakatsuka, and A. P. Coleman, *Orig. Life Evol. Biosp.* **39**, 407 (2009).
- [13] V. S. Letokhov, *Phys. Lett.* **53A**, 275 (1975).
- [14] A. L. Barra, J. B. Robert, and L. Wiesenfeld, *Phys. Lett. A* **115**, 443 (1986).
- [15] Ch. Daussy, T. Marrel, A. Amy-Klein, C. T. Nguyen, Ch. J. Bordé, and Ch. Chardonnet, *Phys. Rev. Lett.* **83**, 1554 (1999); M. Ziskind, C. Daussy, T. Marrel, and Ch. Chardonnet, *Eur. Phys. J. D* **20**, 219 (2002).
- [16] P. Schwerdtfeger, T. Saue, J. N. P. van Stralen, and L. Visscher, *Phys. Rev. A* **71**, 012103 (2005).
- [17] R. A. Hegstrom, D. W. Rein, and P. G. H. Sandars, *J. Chem. Phys.* **73**, 2329 (1980).
- [18] R. Berger and C. Van Wüllen, *J. Chem. Phys.* **122**, 134316 (2005).
- [19] Ľ. Horný and M. Quack, *Mol. Phys.* **113**, 1768 (2015).
- [20] J. N. P. Van Stralen, L. Visscher, C. V. Larsen, and H. J. A. Jensen, *Chem. Phys.* **311**, 81 (2005).
- [21] A. Shee, T. Saue, L. Visscher, and A. Severo Pereira Gomes, *J. Chem. Phys.* **149**, 174113 (2018).
- [22] R. Berger, *J. Chem. Phys.* **129**, 154105 (2008).
- [23] M. Quack, *Chem. Phys. Lett.* **132**, 147 (1986).
- [24] M. Quack, *Angew. Chem., Intl. Ed. Engl.* **28**, 571 (1989).
- [25] M. Quack, *Faraday Discuss.* **99**, 383 (1994).
- [26] M. Quack, *Angew. Chemie Intl. Ed.* **41**, 4618 (2002).
- [27] R. Berger, *Phys. Chem. Chem. Phys.* **5**, 12 (2003).

- [28] J. Sapirstein, in *Relativistic Electronic Structure Theory. Part 1: Fundamentals*, edited by P. Schwerdtfeger (Elsevier, Amsterdam, 2002), p. 468.
- [29] J. A. Pople, J. W. McIver, and N. S. Ostlund, *J. Chem. Phys.* **49**, 2960 (1968).
- [30] F. Pawłowski, J. Olsen, and P. Jørgensen, *J. Chem. Phys.* **142**, 114109 (2015).
- [31] P. Norman, K. Ruud, and T. Saue, *Principles and Practices of Molecular Properties* (Wiley, Chichester, UK, 2018).
- [32] Y. Hao, M. Iliaš, E. Eliav, P. Schwerdtfeger, V. V. Flambaum, and A. Borschevsky, *Phys. Rev. A* **98**, 032510 (2018).
- [33] M. Abe, V. S. Prasanna, and B. P. Das, *Phys. Rev. A* **97**, 032515 (2018).
- [34] M. Denis, P. A. B. Haase, R. G. E. Timmermans, E. Eliav, N. R. Hutzler, and A. Borschevsky, *Phys. Rev. A* **99**, 042512 (2019).
- [35] M. Denis, Y. Hao, E. Eliav, N. R. Hutzler, M. K. Nayak, R. G. E. Timmermans, and A. Borschevsky, *J. Chem. Phys.* **152**, 084303 (2020).
- [36] P. A. B. Haase, D. J. Doeglas, A. Boeschoten, E. Eliav, M. Iliaš, P. Aggarwal, H. L. Bethlem, A. Borschevsky, K. Esajas, Y. Hao, S. Hoekstra, V. R. Marshall, T. B. Meijknecht, M. C. Mooij, K. Steinebach, R. G. E. Timmermans, A. Touwen, W. Ubachs, L. Willmann, and Y. Yin, *J. Chem. Phys.* **155**, 034309 (2021).
- [37] B. Ya. Zel'dovich, D. B. Saakyan, and I. I. Sobel'man, *JETP Lett.* **25**, 94 (1977).
- [38] R. A. Harris and L. Stodolsky, *Phys. Lett. B* **78**, 313 (1978).
- [39] J. Sikkema, L. Visscher, T. Saue, and M. Iliaš, *J. Chem. Phys.* **131**, 124116 (2009).
- [40] L. Visscher, K. G. Dyall, and T. J. Lee, *Intl. J. Quantum Chem.* **56**, 411 (1995).
- [41] L. Visscher, T. J. Lee, and K. G. Dyall, *J. Chem. Phys.* **105**, 8769 (1996).
- [42] Computer code DIRAC, a relativistic *ab initio* electronic structure program, Release DIRAC19 (2019), written by A. S. P. Gomes, T. Saue, L. Visscher, H. J. Aa. Jensen, and R. Bast, with contributions from I. A. Aucar, V. Bakken, K. G. Dyall, S. Dubillard, U. Ekström, E. Eliav, T. Enevoldsen, E. Faßhauer, T. Fleig, O. Fossgaard, L. Halbert, E. D. Hedegård, T. Helgaker, B. Helmich-Paris, J. Henriksson, M. Iliaš, Ch. R. Jacob, S. Knecht, S. Komorovský, O. Kullie, J. K. Lærdahl, C. V. Larsen, Y. S. Lee, H. S. Nataraj, M. K. Nayak, P. Norman, G. Olejniczak, J. Olsen, J. M. H. Olsen, Y. C. Park, J. K. Pedersen, M. Pernpointner, R. Di Remigio, K. Ruud, P. Sałek, B. Schimmelpfennig, B. Senjean, A. Shee, J. Sikkema, A. J. Thorvaldsen, J. Thyssen, J. van Stralen, M. L. Vidal, S. Villaume, O. Visser, T. Winther, and S. Yamamoto, (available at <http://dx.doi.org/10.5281/zenodo.3572669>; see also <http://www.diracprogram.org>).
- [43] T. Saue, R. Bast, A. S. P. Gomes, H. J. A. Jensen, L. Visscher, I. A. Aucar, R. Di Remigio, K. G. Dyall, E. Eliav, E. Fasshauer, T. Fleig, L. Halbert, E. D. Hedegård, B. Helmich-Paris, M. Iliaš, C. R. Jacob, S. Knecht, J. K. Lærdahl, M. L. Vidal, M. K. Nayak, M. Olejniczak *et al.*, *J. Chem. Phys.* **152**, 204104 (2020).
- [44] K. G. Dyall, *Theor. Chem. Acta* **108**, 335 (2002); **115**, 441 (2006); *J. Phys. Chem. A* **113**, 12638 (2009); *Theor. Chem. Acta* **135**, 128 (2016).
- [45] L. Visscher, *Theor. Chem. Acta* **98**, 68 (1997).
- [46] L. Visscher and K. G. Dyall, *At. Data Nucl. Data Tables* **67**, 207 (1997).
- [47] F. Faglioni and P. Lazzeretti, *Phys. Rev. E* **65**, 011904 (2001).